Desalination and Water Treatment
www.deswater.com

doi: 10.5004/dwt.2019.23214

142 (2019) 341–352
February

Degradation of ibuprofen in the photocatalytic process with doped TiO_2 as catalyst and UVA-LED as existing source

Nafiseh Shafeei[a], Gholamreza Asadollahfardi[a,*], Gholamreza Moussavi[b], Masoud Mashhadi Akbar Boojar[c]

[a]*Civil Engineering Department, Faculty of Engineering, Kharazmi University, Tehran, Iran, emails: nafise3721@yahoo.com (N. Shafeei), fardi@khu.ac.ir (G. Asadollahfardi)*
[b]*Department of Environmental Health Engineering, Tarbiat Modares University, Tehran, Iran, email: moussavi@modares.ac.ir*
[c]*Faculty of Biological Sciences, Kharazmi University, Tehran, Iran, email: mboojar@yahoo.com*

Received 27 February 2018; Accepted 28 September 2018

ABSTRACT

Various techniques are available for wastewater treatment. However, some types of pollutants in wastewater need advance treatment such as pharmaceutical components. Advanced oxidation process is one of the most helpful methods to degrade the emerging contaminant like Ibuprofen (IBP). We designed a batch reactor, including light-emitting diode (LED) lamps, TiO_2 and modified TiO_2, to treat synthetic wastewater containing IBP. Our experimental design consisted of 0.5, 2 and 5 mg of IBP, 0.05, 0.1, 0.15 and 0.2, 0.3, 0.4 g of TiO_2 and modified TiO_2, respectively, pH 5, 7 and 9 and exposure time 0.5, 1, 2, 3, 4, 5 and 6 h. We achieved the optimum amount of FeFNCS-TiO_2 and TiO_2 of 0.2 and 0.3 g, respectively, for IBP removal from synthetic wastewater. At pH 7, IBP concentration of 0.5 mg/l and 3 h radiation time, we obtained 91.4% and 52.4% degradation efficiency of IBP from synthetic wastewater in FeFNS-TiO_2/LED and TiO_2/LED processes, respectively. The study of synergistic effects also indicated the positive effect of photocatalyst and LED on each other. The removal efficiency in the FeFNS-TiO_2/LED and TiO_2/LED processes declined by 37.3% and 23.8%, respectively, while adding some amounts of tert-butyl as radical scavenger in the IBP solution. This experiment may indicate the photocatalytic degradation of IBP with the mechanism of hydroxyl radical. We fitted Lagergren's first-order model in a condition, including pH values 7 and 5, 0.5 mg/l IBP concentrations in the synthetic wastewater, 0.2 g of m-TiO_2, 0.3 g of TiO_2 and 1, 2, 3, 4, 5 and 6 h time of exposure. The kinetic rate constant for TiO_2/LED and modified TiO_2/LED were 0.0591 and −0.123, respectively.

Keywords: Ibuprofen removal; Photocatalyst TiO_2; Advanced oxidation process (AOP); Light-emitting diode (LED) lamps

1. Introduction

Nowadays, pharmaceutical compounds which are used as a treatment or prevention are tremendously produced by the companies all around the world [1]. Many recent studies in water and wastewater treatment indicate that pharmaceutical has been entered into the aquatic environment. The concentration of this compound in the aquatic environment is low (with ng/l to μg/l trace level); however, it is considered as an emerging contaminant [2]. In addition to the pharmaceuticals, several other compounds were found as by-products that have been created by a mixture of pharmaceuticals and other pollutants. Also, many other harmful by-products may be found in the future [3].

The most probable way of discharging the pharmaceutical contaminants into the aquatic environment is fluxing via human and animal urine. Therefore, the municipal, hospital and livestock wastewater of pharmaceutical industry can bring the pharmaceutical compounds into the aquatic

* Corresponding author.

1944-3994/1944-3986 © 2019 Desalination Publications. All rights reserved.

environment. In fact, if the pharmaceutical compounds do not contribute to the biological process in wastewater treatment, they enter into the surface water and they may find a way to leak into the ground water [4,5]. Pharmaceuticals as a main group of chemicals can cause to spread out the cancer [6], affect on aquatic growth [7] and defect the male's genital system and change undesirably in the physiology of the animals [8]. The pharmaceuticals fall into several groups. Nonsteroidal anti-inflammatory drugs (NSAIDS) are the first and most important types of pharmaceuticals. Anticonvulsants, antibiotics and lipid regulators are the other classes of pharmaceuticals [3]. Ibuprofen (IBP) is an NSAIDS pharmaceutical known by the [2-(4-2-methylpropyl) phenyl] propionic acid name and $C_{13}H_{18}O_2$ formula. They are mostly used as a pain relief and in fever reduction [7,9].

Recently, many studies have been conducted around the world, which demonstrated existing of IBP in the water supplies. In Korea, IBP was found in surface, drinking and wastewater [10]. The IBP was discovered in surface and treated water of Louisiana, USA, and Ontario, Canada [11]. An investigation indicated that west prong little pigeon river's water contains IBP [12]. In UK, the presence of IBP in River Tyne was investigated [13]. Buser et al. explained that influents of the IBP concentration from three wastewater treatment plants were between 0.99 and 3.3 μg/l [14]. Herberer et al. reported that the IBP concentration in sewage effluent was about 0.22 μg/l in Germany [9]. Another study in USA indicated that the IBP concentration in raw and reclaim water was between 0.9 and 2.11 μg/l. The amount of IBP in the effluents of numerous of treatment plants was stated to be between 0.002 and 24.6 μg/l [15].

Adsorption, membrane [16] and advanced oxidation process (AOP) have recently been used for pharmaceutical removal from aquatic environments [17]. The presence of pharmaceuticals in treated water indicated that the conventional techniques in water and wastewater treatment plants are not able to remove this pollutant completely [11]. In AOPs, the pollutants can be decomposed with the reaction in which receiving and releasing of electron occurs between reactive and photocatalysts [2]. Photocatalytic oxidation (PCO) is a kind of AOP in which hydroxyl radical, one of the reactive sorts produced in AOPs, is rather potent. PCO is conducted via artificial or natural UV ray and photocatalyst [18]. The photocatalytic mechanism using UV and photocatalyst TiO_2 is such that when the photocatalyst is exposed to radiation photons whose energy is equal to or larger than the bandgap photocatalyst, the electrons in the valence band, existing in photocatalyst atom, absorb the energy and are stimulated. Then they transmit to the conduction band at higher energy levels. At the same time, a number of electrons and cavities are created in the photocatalyst atom. Thus, the oxidation of oxygen by electrons and the oxidation of organic matter are caused by the interference of the generated cavities, and the organic matter decomposes through a series of oxidation and reduction reactions to the intermediate products [19]. Photocatalytic processes, considering the importance of using solar energy as a source of energy, more environmental friendly [20,21], renewable energy [22], fast oxidation, higher efficiency and the lack of multi-ring by-products [23], are preferable to other purification methods.

AOP is mostly investigated in pharmaceutical removal. Photodegradation of IBP by UV light in the aquatic environment [24], heterogeneous photocatalysis by TiO_2 and UV [25] and photocatalytic degradation of IBP by TiO_2/UVC and TiO_2/UVA [26] were previously studied. Mercury lamps have been used as a UV source in most of the photocatalytic degradation, but today it started gradually to employ light-emitting diodes (LEDs) instead of mercury lamps. Because the LED lamps have lower toxicity than mercury lamps, as well as longer useful life span and more flexibility. Therefore, substitution of the LED lamps instead of mercury lamps may be a suitable alternative [27].

As mentioned previously, photocatalyst is one of the most important components in PCO. TiO_2 is a nontoxic, cut-rate and powerful catalyst with a 3.0–3.2 eV bandgap. Modifying the TiO_2 has considerable effects on the performance of photocatalyst reactor. The most important effect is improving the photocatalytic activity [28]. In recent years, several studies have investigated the effect of doping TiO_2 by metals and nonmetals such as Fe, F, N, S and C [18,25,27].

Because IBP is considered to be an emerging contaminant and its health standard does not exist in the world, many of the effects, as well as side effects, of its interaction with other pollutants are unknown. Removing this pollutant from water is vital. On the other hand, because of the disadvantages of mercury lamps, its replacement with LED lamps in photocatalytic processes can have a particular significance.

The objective of this study was to determine IBP, (RS)-2-(4-(2-methylpropyl)phenyl)propanoic acid, removal efficiency from synthetic wastewater by applying photocatalytic batch reactor including FeFNS-TiO_2 and UV-LED lamps. The effect of pH variation, photocatalyst concentrations, IBP concentration and exposure time on removal of IBP was considered.

2. Materials and methods

2.1. Experimental setup

We made a batch reactor, which consisted of a glass saucer with a volume of 100 ml. A UV-LED circuit was assembled on an aluminum plate that was stuck under the heat sink with the sides 11.2 × 12 cm. To cool the heat sink, a fan was mounted on the heat sink. The UV-LED circuit was installed in a circle aluminum plate with a radius of 4.85 cm. Eighteen UV-LED lamps were regularly installed in two concentric circles with the radius of 43.5 and 21 mm, respectively. The circuit turned on and off with 2 switch powers placed beside the heat sink. The characteristics of each UV-LED bulb included bulb length of 45 mm, bulb diameter of 45 mm, angle of radiation of 120°, intensity of 320 mA and wavelength of 365 nm. The bulbs were made by Seoul semiconductor, South Korea. We used DC power supply via 2 drivers with the intensity of 320 mA and 24–25 volts. Potential difference was between 3.2 and 3.4 volts. All the experiments were conducted in the batch reactor with the capacity of 100 ml and the radius of 5 cm built from glass to facilitate the experiments of IBP degradation. Fig. 1 indicates the schematic of the batch reactor in our study.

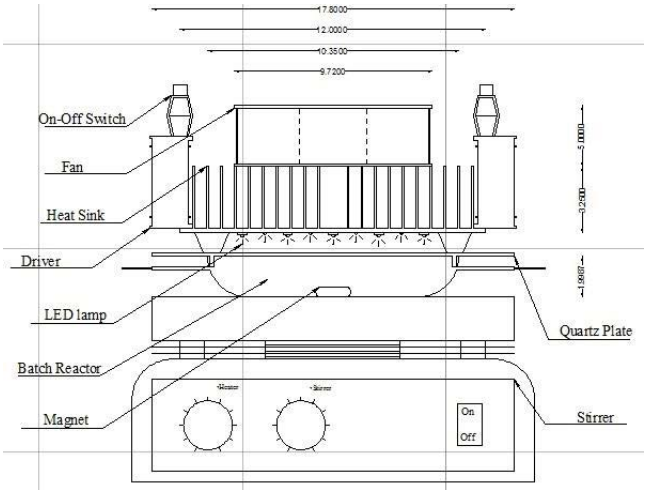

Fig. 1. A schematic picture of the batched reactor.

The stirrer was switched on during the irradiation. To prevent the UV-LED bulbs from contact with the contents of the batch and its vapors, a quartz plate was placed between the batch and the UV-LED bulbs. The distance between aluminum plate and the surface of the sample in the reactor was 10 mm.

2.2. Experimental procedure

We used TiO_2 and FeFNS-doped TiO_2 (called m-TiO_2) nanocatalyst for the experiment. Both of these materials were synthesized by a cell-gel method. To produce the TiO_2, 6 ml of titanium (IV) butoxide was dissolved in 17 ml of 2-propanol. The first solution mark was tagged on it. A second solution was prepared by increasing the pH equal to 2 by using glacial acetic acid. After that, the first solution was slowly dropped into the second solution [29]. The final solution was rigorously mixed by a stirrer for 2 h. Then the prepared mixture was put in a dark room for 48 h. The solution's pH was measured and because the pH was less than 3, we added ammonia to the solution until the pH reached 3. The final powder was obtained by drying the solution at 80°C and calcinating it in 500°C for 3 h [18].

To prepare FeFCNS-doped TiO_2, 3.8 g thiourea was dissolved in deionized water. A temperature condition of 4°C–6°C was highly needed to prevent a probable reaction and by-product generation [30]. After mixing the solution, 7.32 ml of $FeCl_3$, H_2O, titanium (IV) butoxide were added and a heterogeneous suspension was obtained. We achieved a creamy solution when the suspension was stirred for 12 h. To dope final solution with the fluorine, a 30 μl fluorine acetic acid was added. The creamy solution was kept in an immobile state and a dark room. Afterward, the FeFCNS-doped TiO_2 powder was obtained by drying the solution in 80°C and then calcinating it in 475°C [31].

We synthesized the catalyst according to the procedure of Hossiani et al. [18]. We determined the catalyst characteristics such as specific surface, the size and crystalline phase, morphology of the surface and the photo-physical properties. The size and volume of pores were precisely analyzed. The crystalline phase of the catalyst was determined using X-ray diffraction (XRD) analysis [18]. The intensity and the voltage of XRD diffractometer were fixed at 30 mA and 40 kv, respectively. CuKa radiation was employed in the radiation angle between 10°C and 80°C. Specific area, size of pores and also their volume were determined with the N_2 adsorption and desorption [32].

2.2.1. The photocatalyst characterization

We carried out the XRD analysis to determine the crystalline phase of photocatalyst and prepared the TiO_2 catalyst according to the study by Hossaini et al., except that our calcination temperature, drying temperature and drying time were not the same [18]. Some other information we extracted from XRD patterns such as the average size of crystals can be determined using Eq. (1).

$$D = \frac{K\lambda}{\beta \cos\theta} \tag{1}$$

where λ is the wave length of XRD pattern (CoKa radiation) and β is the width of the graph at the half of maximum intensity. K is constant equal 0.9 and θ is the angle of diffraction. A scanning electron microscope (SEM) test was used to observe the morphology of photocatalysts. We determined the surface and pore characterization of the catalysts using Brunauer–Emmett–Teller (BET) analysis. We plotted N_2 adsorption isotherm. We used energy-dispersive X-ray analysis (EDX) to identify the presence of dopant elements in m-TiO_2. Fourier transform infrared spectroscopy (FTIR) analysis was performed to identify the functional groups (chemical property of the compound) and connections in the compound. To determine the precise dimensions of nanoparticle photocatalysts, we used the transmission electron microscopy (TEM) analysis, and it was proved from TEM figures that the nanoparticles had the size range of 1–100 nm.

One of the most important factors in photocatalysis is a photocatalyst bandgap. The bandgap can be calculated using Eq. (2).

$$E_{ev} = \frac{1.24}{\lambda(\mu m)} \tag{2}$$

where E is bandgap energy (eV) and λ interrupt wavelength (nm).We calculated the bandgap of m-TiO_2 and TiO_2 by using Eq. (2). The bandgap (E) for m-TiO_2 and TiO_2 were 3.03 (eV) and 3.20 (eV), respectively [18]. These amounts prove that m-TiO_2 can be stimulated by lower energy. It means m-TiO_2 is more absorbent of photon energy to generate electron holes and hydroxyl radicals participating in photocatalysis. In fact, the m-TiO_2 can produce more hydroxyl radicals to degrade of pollutant.

2.3. Sample preparation

To prepare synthetic wastewater, the water contaminated with IBP artificially, we dissolved 400 mg of IBP in 1 l of deionized water to obtain sample for our experiment.

For access to selected concentration, the defined volume of IBP solution was mixed with the required volume of deionized water. The quantity of water and IBP solution for mixing was calculated by dilution. Afterward, the prepared solution was poured into the batch reactor (Fig. 1) and the nano-photocatalyst was added into the solution. Finally, the batch put on the stirrer and the contents of the reactor were irradiated with UV-LED bulbs for the time mentioned in the design of the experiment (Table 1).

We measured adsorption of catalyst by performing the test without any bulbs and in the dark condition. The obtained sample was passed through a syringe 0.2 μm filter. To determine the UV-LED degradation, the same test was done by UV-LED bulbs without any nano-photocatalyst. We injected the final samples into high-performance liquid chromatography (made by HACH). We changed pH, pollutant concentration, photocatalyst concentration and time in all the experiments to assess the condition in which the highest IBP removal from polluted water occurred. The pH of the solution was increased by adding NaOH solution and measured by a pH meter (Model HQ40D, USA).

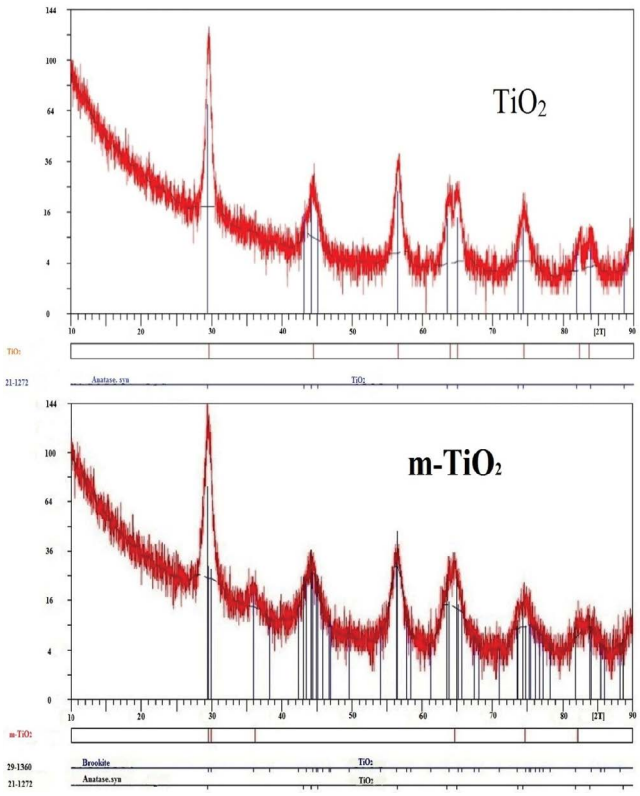

Fig. 2. The XRD analysis of TiO_2 and m-TiO_2 elements.

3. Result and discussions

3.1. Characterization of photocatalysts

As indicated in Fig. 2, the intense diffraction peak occurred in diffraction angles of 29.44°, 44.19°, 56.42°, 63.49°, 64.92° and 74.33°. The similarity between diffraction angles of TiO_2 and m-TiO_2 was related to their ingredient because the dopant metal and nonmetal in m-TiO_2 was not enough to change its diffraction angle and they can just effect on properties which enhance the photocatalytic activity. The commercial TiO_2 may have different peak in XRD pattern. Hossaini et al. indicated diffraction angles of 31.83, 41.86, 47.82, 51.30, 63.01, 65.7 and 72.78 for TiO_2 [18].

In Fig. 2, the vertical axis indicates the intensity of the reflected beam per second (cps) and the horizontal axis is the angle between the radiated and the reflected beam (°).

As presented in Fig. 2, we observed anatase phase in TiO_2 catalyst. However, in m-TiO_2 powder, Brookite phase and anatase phase were observed (Fig. 3). The peak of the Brookite phase in m-TiO_2 did not arise because the nonmetal dopant has a repressive property in phase convert. An investigation in crystallinity of TiO_2 and m-TiO_2 proved that adding some metal dopant into TiO_2 can make the crystal to be more regular [33]. We obtained the catalyst size for m-TiO_2 and TiO_2 equal to 6.4 nm and 13.97 nm, respectively. As mentioned previously, doping the photocatalyst with metal and nonmetal increases the crystal size.

Several studies that reported the XRD pattern of different samples exist. Our result can be supported by these studies. In the present work, similar to the work of Naushad et al. and Pathania et al., because of the quasicrystalline nature of the material, the peaks are quite distinct, but in both of these, due to the lesser distance between the crystalline plates, the peaks occur at a lesser angle [34,35].

These diffraction angles are very close to the Ni-TiO_2 diffraction angle element in Rajendran's work. The difference between the angles obtained in our study for pure TiO_2 and the angles obtained in Rajendran's work is at most less than 1° [36].

The obtained XRD diagram, such as the Pathania diagram, is a graph between amorphous graphs and regular crystalline materials. This indicates that the generated photocatalysts, such as GG/AO, are composed of more than one phase. Also, due to the difference in the distance between the crystalline plates, the photocatalyst diffraction angles made in this study are slightly less than that in the study by Pathania et al. [37].

Table 1
Design of the experiment

pH	5, 7, 9	5, 7, 9
IBP concentration (mg/l)	0.5, 2, 5	0.5, 2, 5
Catalyst concentrations (g)	0.05, 0.1, 0.15, 0.2, 0.3, 0.4	0.05, 0.1, 0.15, 0.2, 0.3, 0.4
Time (h)	0.5, 1, 2, 3, 4, 5, 6	0.5, 1, 2, 3, 4, 5, 6
Photocatalyst	m-TiO_2	TiO_2

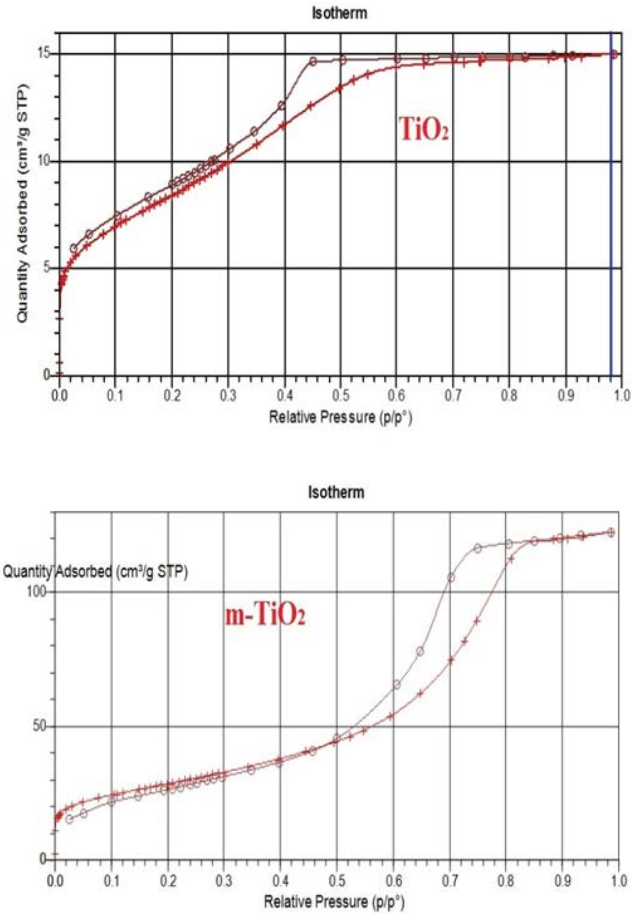

Fig. 3. Adsorption isotherm of TiO_2 and m-TiO_2.

In our XRD diagram, as in the XRD diagram of Kumar's work, the peaks connect with a curved path that indicates the multiphase of the elements. The difference in the radiation intensity of the elements is due to the difference in the atomic number of the elements. Due to the lower atomic number, the combination of g-C_3N_4 has less intensity than TiO_2 [38].

As illustrated in Fig. 3, both photocatalyst isotherms are related to a porous material and they follow isotherm type VI. The surface and pore characterization of the catalysts were determined using the BET analysis. The surface areas of m-TiO_2 and TiO_2 were 110.5 and 43.5 m^2/g, respectively. We observed volume of 0.044 and 0.014 cm^2/g for m-TiO_2 and TiO_2 pores, respectively. The commercial TiO_2 has a surface area in the range of 85–120 cm^2/g. Fig. 5 indicates the surface and pore characterization of m-TiO_2 catalysts using the BET analysis.

The difference between specific surface and the rate of porosity, which was obtained in our study and in the work by Hosseni et al. [18], may be caused by differences between time of calcination and drying time of two studies. Drying time and calcination temperature of Hosseini et al. were 24 h and 380°C, respectively. However, drying time and calcination temperature in our study were 48 h and 500°C, respectively. The difference between the surface area and pore volume of commercial TiO_2 with TiO_2 made in our study may be related to different preparation methods.

Fig. 4 indicates the morphology of TiO_2 and m-TiO_2 using SEM analysis. The surface area in doped TiO_2 increased because of its bigger crystal. According to magnification of images, both m-TiO_2 and TiO_2 particles are in nanoscales. The nanoparticles also have a clear surface with partly round particles.

To obtain the size range and exact dimensions of the m-TiO_2 and TiO_2 photocatalytic nanoparticles, TEM analyses were performed. As indicated in Fig. 5, the sizes of TiO_2 and m-TiO_2 particles are measured at 40, 60 and 100 nm by chance.

We tested the EDX to confirm that the presence of elements are necessary for modifying nanoparticles of titanium. Fig. 6 indicates the existence of Fe, F, C, N, Ti and O in titanium dioxide and modified titanium dioxide.

As indicated in Fig. 7, the functional groups of O–H, C–N, C–H and N–O are recognized in TiO_2 compound. O–H, C–N, C–C and C–O are also observed as some functional groups in m-TiO_2. The functional groups have the main effect of photocatalyst characteristics.

By comparing the FTIR spectrum and the wavelength of each peak in the present work, it can be found that the wavelength of 3,410.23 belongs to the O–H [35] bond, 1,626.75 belongs to the C–O bond, 1,626.75 belongs to C–C [34], 1,534.50 belongs to the C–N [38] bond and 1,455.43 belongs to the transplant C–H [37].

3.2. Photocatalytic activity

We attempted to improve the photocatalytic activity of TiO_2 by doping it with Fe, F, N, C and S. All of the metal and nonmetal elements used for doping had a specific function in photocatalysis, so that the surface oxygen holes form when F is added, improving the crystallinity and stronger absorption in the UV-visible range [32]. The existence of Fe in doped TiO_2 can help electron holes and hydroxyl radical to be produced. Doping of TiO_2 with N-S also increases the light absorption [31]. In addition to the proposed relationship in calculating the bandgap, which is a unique photocatalystic property, this photocatalyst characteristic can be measured using diffuse reflectance spectra analysis of any photocatalyst. Based on the work of Hosseini et al., the TiO_2 and m-TiO_2 photocatalyst bandgaps obtained using the proposed Eq. 2 (ev) were 3.2 and 3.03, respectively. The difference between TiO_2 and m-TiO_2 photocatalyst bandgaps indicates that m-TiO_2 requires less energy than TiO_2 for being stimulated [18]. We indicated that the photocatalytic activity of doping TiO_2 is much more than TiO_2. On the other hand, doped TiO_2 had a smaller crystal, more light absorption, larger pores and lower bandgap compared with TiO_2, so that it can be more active in photocatalytic reactions. We removed IBP in batch reactor, including m-TiO_2/LED and TiO_2/LED PCO. We studied the effect of pH, time, photocatalyst concentration and IBP concentration in the removal of IBP from polluted water for which the results are as follows:

3.3. Effect of pH

Removal of IBP from synthetic wastewater had a different behavior in acidic, natural and alkaline pH. We attempted to investigate the IBP removal from polluted water in three pH

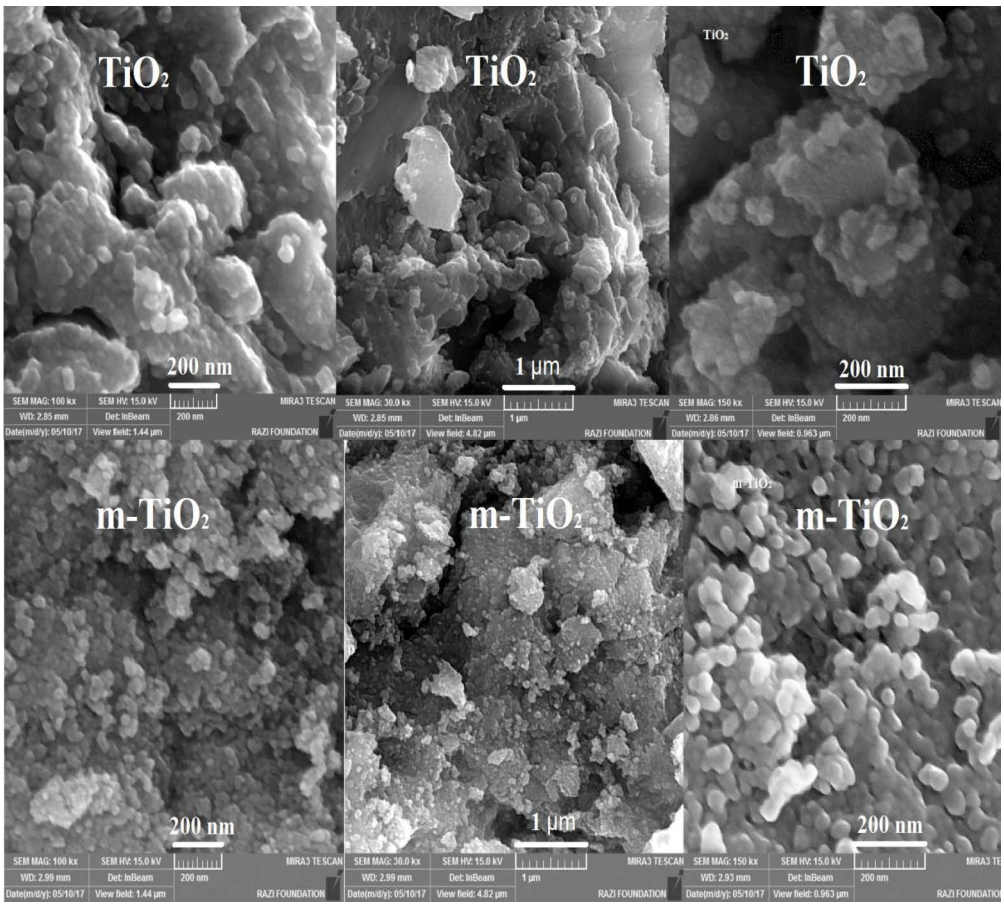

Fig. 4. SEM image showing morphology of TiO_2 and m-TiO_2.

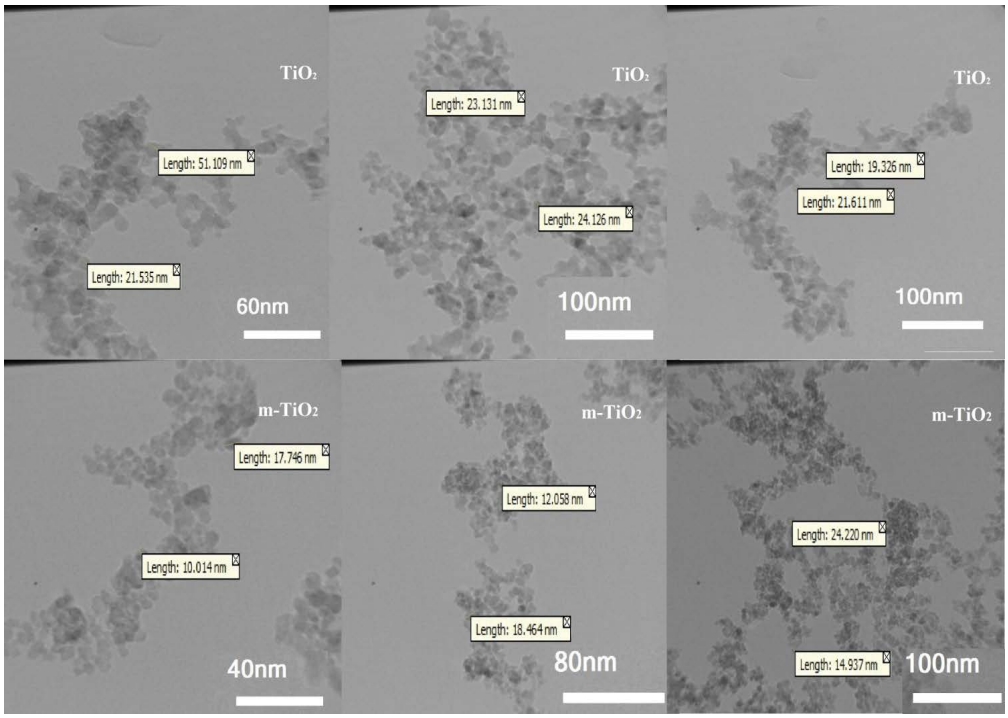

Fig. 5. TEM analysis of TiO_2 and m-TiO_2.

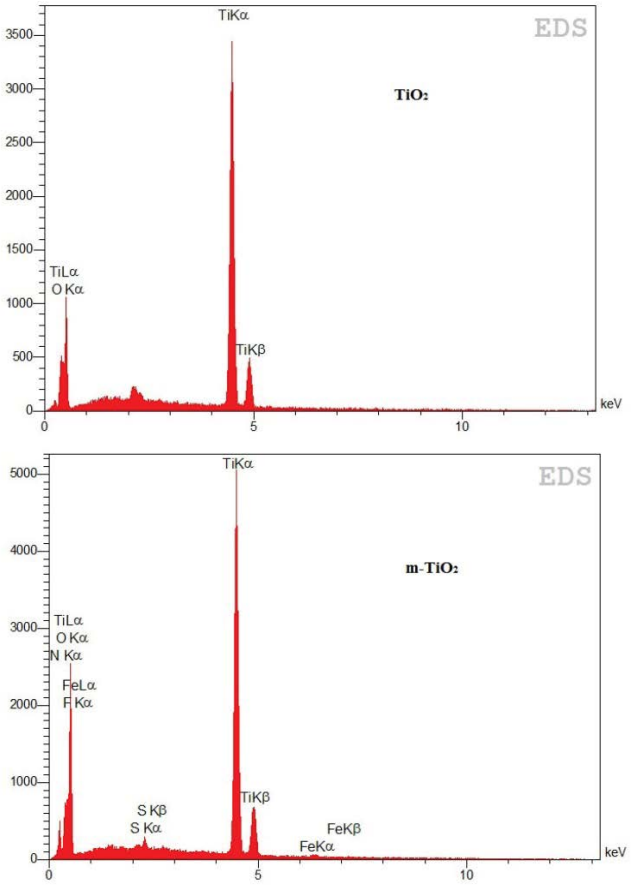

Fig. 6. Analysis of pure and modified TiO_2 (m-TiO_2) elements (horizontal axis: released an amount of energy (keV), vertical axis: intensity (a.u.)).

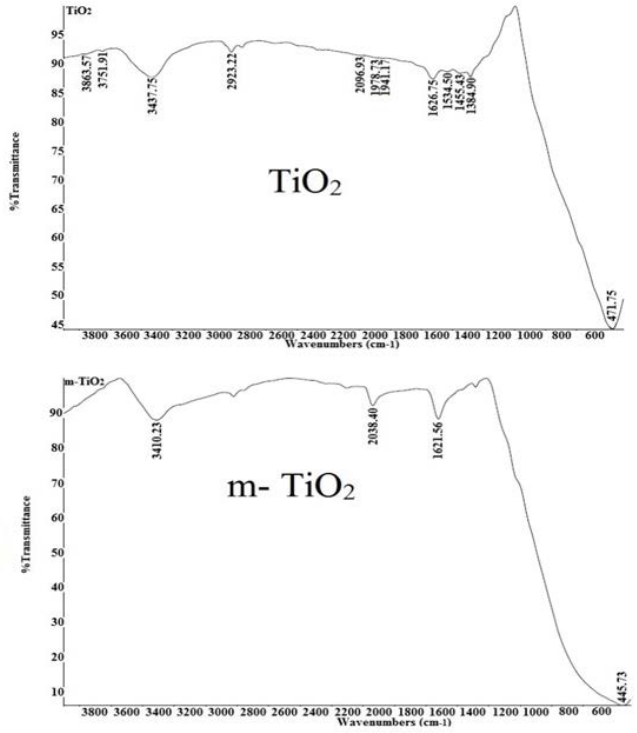

Fig. 7. FTIR analysis for m-TiO_2 and TiO_2.

values: 5, 7 and 9. We conducted experiments with an IBP concentration of 5 mg/l, in a 5-h time of exposure and 0.1 g catalyst. Fig. 8(a) indicates the results of IBP removal from a synthetic wastewater. As presented in Fig. 8(a), we achieved 31%, 37.5% and 18.4% IBP removal at pH values 5, 7 and 9, respectively, while applying m-TiO_2/LED as a photocatalyst in the batch reactor. However, we obtained 24.2%, 21% and 14.6% IBP removal from polluted water at pH values 5, 7 and 9, respectively, while using LED/TiO_2 PCO in the batch reactor (Fig. 8(a)).

Fig. 8(b) presents the results of IBP removal from synthetic wastewater at pH values 5, 7 and 9, respectively, while applying only m-TiO_2 and TiO_2 in the batch reactor. We carried out experiments with an IBP concentration of 5 mg/l, 0.1 g photocatalyst and in a 5-h time of exposure. As illustrated in Fig. 8(b), the highest IBP removal from synthetic wastewater occurred at acidic pH while only m-TiO_2 catalyst was used. When we applied TiO_2 as a catalyst in the batch reactor for IBP removal from synthetic wastewater, the efficiency at neutral pH = 7 was higher than that for other pH. Ionvio et al. indicated that the highest removal of IBP under UV radiation was achieved at acidic pH [24].

The results of the pH effect on the efficiency of the adsorption system depend on pHpzc (pH at the isoelectric point) of the photocatalyst. Since the pHpzc value of TiO_2 photocatalyst and its modifications are within the acid and neutral pH ranges [39] and IBP also contains polar carboxyl group (COOH), in acidic and neutral conditions, the absorption of pollutants is easier and more efficient [40].

3.4. Effect of time in removal of IBP in polluted water

To determine the effect of time in the removal of IBP from synthetic wastewater, we changed the time of experiment from 30 min to 6 h. We also performed experiments with 5 mg/l IBP and 0.1 g photocatalyst. Fig. 9 presents the effect of time in the removal of IBP from synthetic wastewater.

As presented in Fig. 9, by increasing the time, the removal of IBP from polluted water increases. In m-TiO_2/LED and TiO_2/LED photoreactors, the removal of IBP from synthetic wastewater increased until it reached to the maximum amount. We achieved the maximum efficiency of removal of IBP from polluted water by 50%, 37.2% and 8.2% in 360 min for m-TiO_2/LED, TiO_2/LED PCOs and LED, respectively. Removed IBP by LED only and m-TiO_2 only also increased with a low rate, which were 5.5% and 3.95%, respectively.

As indicated in all of the test procedures, by increasing the exposure time, the removal rate increases both in the adsorption and in the photocatalyst process, due to the greater exposure of the pollutant to the photocatalyst and the longer radiation.

3.5. Effect of photocatalyst concentrations

We changed the amount of photocatalysts during our experimental work. We also carried out experiments with 5 mg/l IBP. As indicated in Fig. 10, the maximum removal

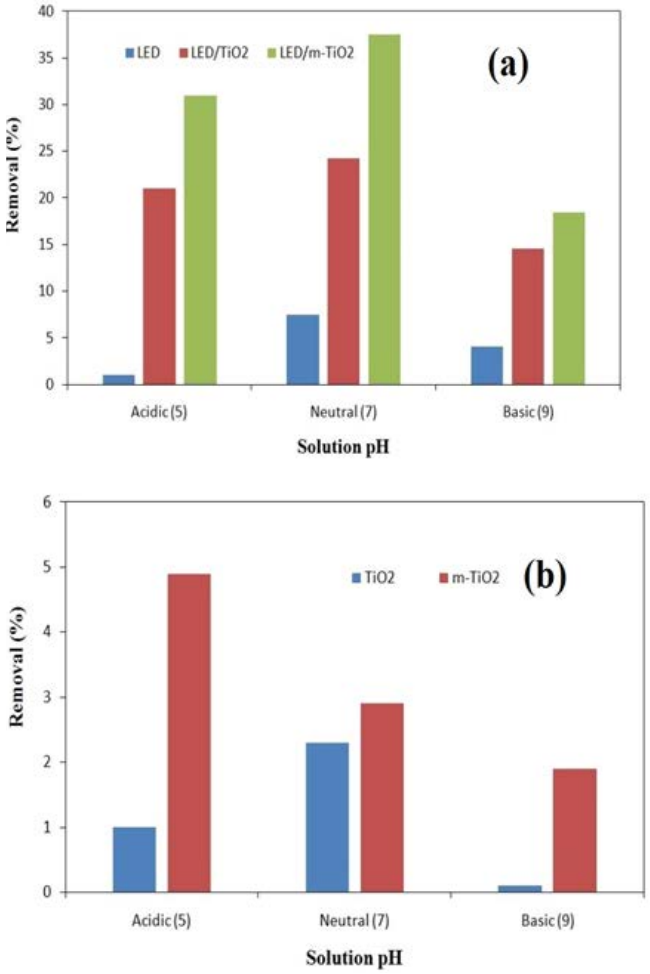

Fig. 8. IBP removal percentages of synthetic wastewater at different pH (5 mg/l IBP concentrations and 0.1 g catalyst).

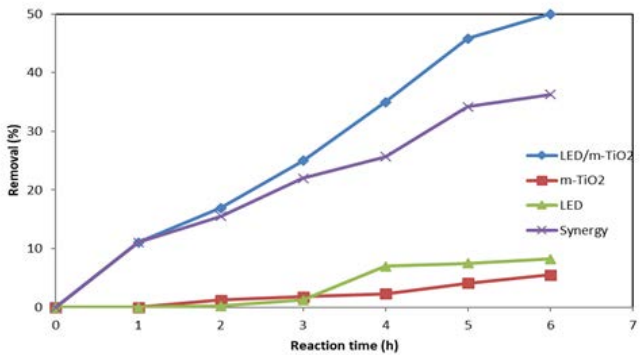

Fig. 9. Effect of time in removal of IBP in the polluted water.

efficiency of IBP from synthetic wastewater occurred at a concentration of 0.3 g for m-TiO_2 and 0.2 g for LED/m-TiO_2. Fig. 10 also presents maximum removal efficiency at 0.3 g for LED/TiO_2 and 0.4 g for TiO_2. We reached 34.4% and 45.8% IBP removal efficiency for TiO_2/LED and m-TiO_2/LED PCOs, respectively. While the amount of catalyst in the reactor increased, the polluted water in the reactor changed to

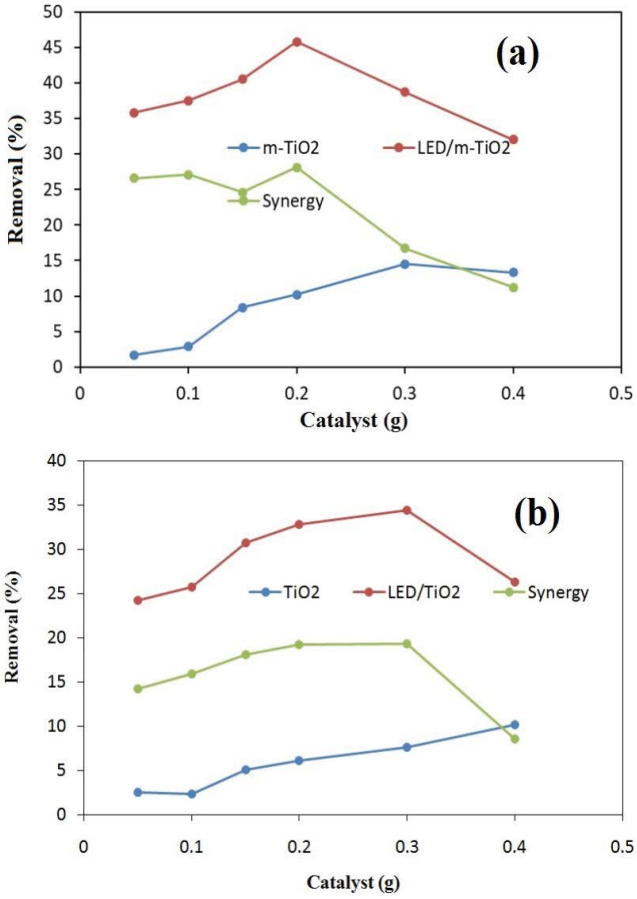

Fig. 10. The removal efficiency of IBP from synthetic wastewater with different amounts of catalyst.

cloudy water and caused to scatter the LED light radiation in the reactor. As a result, the IBP removal efficiency decreased. Therefore, increasing the amount of photocatalysts do not necessarily increase the removal efficiency. It can cause to increase the removal efficiency until the photocatalyst amount reaches to an optimum value of photocatalyst.

In fact, the removal efficiency decreased at both very high and very low concentrations of the photocatalyst and the most efficient removal occurred at optimum concentrations of m-TiO_2 and TiO_2. We carried out all these experiments with 5 mg/l IBP concentration at the natural pH (7). In all tests, the polluted water was irradiated for 5 h. We also observed that the optimum amount of m-TiO_2 used in our experiment is less than TiO_2. It means that in a similar condition, m-TiO_2 is effective than TiO_2 to remove IBP from polluted water.

3.6. Effect of IBP concentrations

The IBP removal was severely affected by changing IBP concentration. The removal efficiency increased by reducing the IBP concentration. We selected polluted water with 0.5, 2 and 5 mg/l of IBP concentrations to demonstrate the concentration effect.

Fig. 11 presents removal efficiency of IBP while using TiO_2/LED with 0.3 g of catalyst and m-TiO_2/LED with 0.2 g of catalyst, including 2 mg/l IBP in solution. As presented in

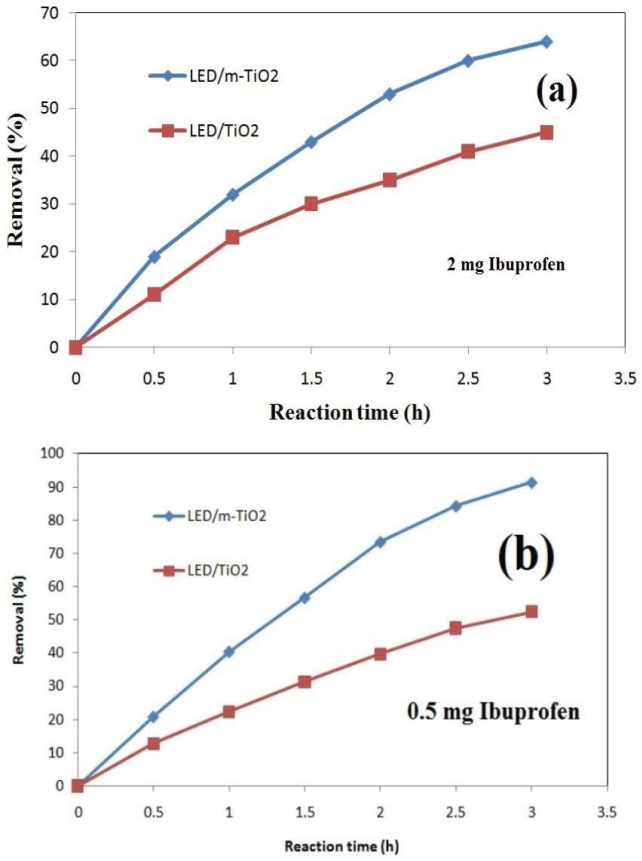

Fig. 11. Removal efficiency of 0.5 and 2 mg/l IBP from polluted wastewater.

Fig. 11, the maximum removal was 64% and 45% for using m-TiO_2/LED and TiO_2/LED PCOs, respectively, in 3 h. As indicated in Fig. 11, the maximum removal of IBP from synthetic wastewater occurred while we used 0.5 mg/l IBP in our batch reactor. The removal efficiency was 91.26% and 52.4% for m-TiO_2/LED and TiO_2/LED PCOs, respectively. We performed our experiments in a period of 1–3 h, and the most treatment occurred at 3 h.

3.7. Photocatalyst potential

To better understand the effect of doping TiO_2 by F, Fe, N, S, we used Eq. (4) to obtain the catalytic potential [18].

$$R_{obs} = R_{pco} - \left(R_{ads} + R_{LED}\right) \tag{3}$$

where R_{obs} is the degradation efficiency in photocatalytic removal with photocatalyst and LED, R_{LED} is the degraded performance without any photocatalyst and under the LED radiation and R_{ads} is the adsorption by photocatalyst. The R_{obs} is synergy efficiency, which we drew in some of the figures.

As clarified in Fig. 8, when 50% of dissolved IBP was removed by m-TiO_2/LED PCO and 5.5% of IBP adsorbed by m-TiO_2 (in a dark condition) and also 8.2% of IBP eliminated under LED without any photocatalyst, we obtained R_{obs} equal to 36.3%. It means photocatalyst and LED can reinforce each other in the photocatalysis.

3.8. Kinetic studies of IBP removal in TiO_2/LED and m-TiO_2/LED PCOs

In our experiments, the removal efficiency was a function of time. We used Langergren first-order kinetic model according to Eq. (5)

$$\ln\left(\frac{C_t}{C_0} = -K_{appt}\right) \tag{4}$$

where C_t is the IBP concentration in the synthetic wastewater at the time t. C_0 is the initial concentration of IBP in the synthetic wastewater and K_{app} (1/d) is the rate of adsorption of IBP which is constant during photocatalysis. We fitted Lagergren's first-order model in an optimal condition, including pH values 7 and 5, IBP concentration of 0.5 mg/l in the synthetic wastewater, 0.2 g of m-TiO_2, 0.3 g of TiO_2 and 1, 2, 3, 4, 5 and 6 h time of exposure (Fig. 12). The kinetic rate constant for TiO_2/LED and m-TiO_2/LED were 0.0591 and −0.123, respectively. As indicated in Fig. 12, the coefficient of determination (R^2) between the experimental results and Lagergren's first-order model, while using TiO_2/LED, is 0.9799, which means the data follow Lagergren's first-order model. While we applied Lagergren's first-order model for the m-TiO_2/LED, the R^2 between the experimental results and Lagergren's first-order model is 0.9809, which indicate a good agreement exists between experimental data on the model.

Numerous studies were performed to remove emerging contaminants, such as IBP. Present research has some differences and advantages. Table 2 indicates differences between the present study and previous works.

3.9. Mechanism of the PCO

3.9.1. The effect of tert-butyl radical scavenger on the photocatalytic removal of IBP from aqueous solution in the UV-LED / m-TiO_2 process

The mechanism for removing contaminants through advanced oxidation reactions is based on oxidation using free hydroxyl or free radicals. Because the OH• is the most

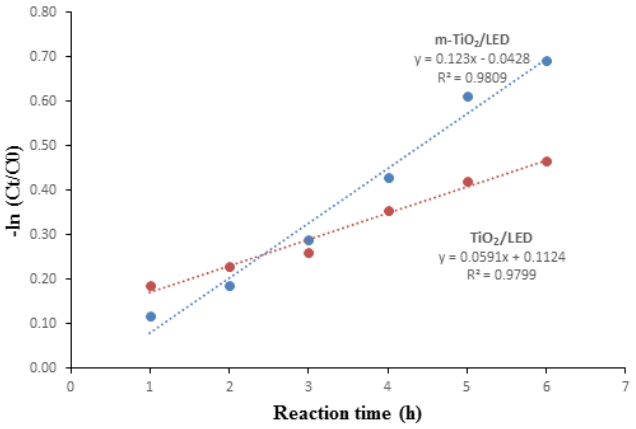

Fig. 12. The kinetic decomposition of IBP of the synthetic wastewater in the process of using TiO_2/LED and m-TiO_2/LED.

Table 2
Comparison between pervious study and present work

Authors	Research topic	Result	Comparison with present study
Kanakaraju et al. [41]	TiO_2 photocatalysis for pharmaceutical wastewater treatment	Degradation of IBP using solar UV-A irradiation in pure water and TiO_2 is efficient for IBP degradation	The difference in the current work is the source and photocatalyst type. We replaced the light source with a lower energy consumption (LED) and photocatalyst with a higher photocatalytic activity.
Georgaki et al. [42]	A Study of the Degradation of Carbamazepine and IBP by TiO_2 & ZnO Photocatalysis upon UV/Visible Light Irradiation TiO_2 & ZnO Photocatalysis upon UV/ Visible-Light Irradiation	TiO_2 photocatalysis upon UV/visible light irradiation had 100% removal efficiency	The difference in the current work is the source and photocatalyst. We replaced the light source with a lower energy consumption (LED) and photocatalyst with a higher photocatalytic activity.
Papamija et al. [43]	Photocatalytic Degradation of IBP Using Titanium Dioxide	After this investigation, 80.64% degradation of IBP was achieved.	The difference between our work and the study by Papamija et al. was in energy source and the type of photocatalyst, as explained earlier, we attempted to improve its profile. The number of variables used in our work was greater than that in the work of Papamija et al.
Braz et al. [28]	Photocatalytic Degradation of IBP using TiO_2	Degradation of IBP by UV-TIO_2 occurred after 60 min and it was found that these pores are efficient for IBP removal.	They used mercury lamps and just the effect of the pH variable on the basis of a simple TiO_2. We replaced the mercury lamps with the LEDs to reduce the energy consumption and toxicity of mercury lamps and examined more variables and the photocatalysts were modified to enhance the photocatalytic activity
Silva et al. [26]	Photocatalytic degradation of IBP by TiO_2/UVC and TiO_2/ UVA	The TiO_2/UV-C system had more removal efficiency than a TiO_2/UV-A system for removing the IBP and the TiO_2/ UV-C could completely remove the pollutant.	We replaced the mercury lamps with the LEDs to reduce the energy consumption and toxicity of mercury lamps. We also achieved more efficiency by modifying the photocatalyst and using UV-A
He [44]	IBP removal using H_2O_2 and UV radiation		Our catalyst is different from study by He and our source energy is different.

important component of photocatalysis, the photocatalytic degradation decreases as $OH^{\bullet}$ reduces. The tert-butyl chloride radical scavenger effects were investigated on the removal of water-soluble IBP. This material reduces free radicals by using radicals in the solution of the test. This radical scavenger was added to the solution at a concentration of 0.1 mM. As indicated in Fig. 13, the presence of tert-butyl chloride radical as a scavenger decreases the efficiency of IBP removal by about 41% in the UV-LED/m-TiO_2 and by about 36% in the UV-LED/ TiO_2. This indicates that the IBP oxidation mechanism is done with the help of free radicals. Therefore, based on this claim, if the amount of free radicals in the system is reduced, the process efficiency should also be reduced. According to the results, adding a few radical scavenger to the system reduced the efficiency of removal, which indicates that the removal of IBP occurred by advanced oxidation mechanism before adding radical scavengers [24]. For example, the efficiency of the m-TiO_2/LED process is about 48.5% without the presence of radical scavengers and in the test conditions, which was reduced by adding radical scavenger to 8%.

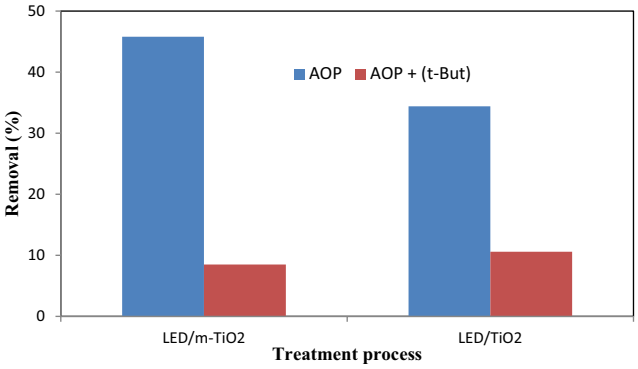

Fig. 13. The effect of tert-butyl radical additive on photocatalytic removal of IBP from polluted aqueous solution in the UV-LED/m-TiO_2 process.

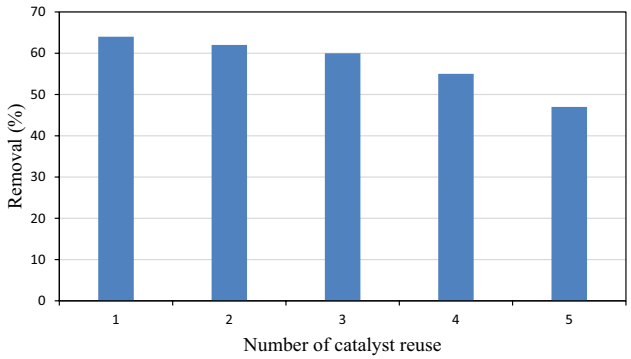

Fig. 14. Recyclability of m-TiO_2.

3.10. Recyclability of nanoparticles

Khaleghi Abbasabadi et al. studied the recyclability of TiO_2 nanoparticles. They recovered the TiO_2 nanoparticles and then reused it for 3 cycles, and it was proved that TiO_2 nanoparticles can perform as a photocatalyst without significant reduction in efficiency. They achieved 80%, 78%, 75% and 75% efficiencies for 1, 2, 3 and 4 recovering cycles, respectively [45].

For investigating the recyclability of nano-doped TiO_2 nanoparticles, we conducted the recycling and reusing tests for this catalyst. All the tests were conducted in the same condition. The catalyst amount of 0.2 g, pollutant concentration of 2 mg/l and 3 h of exposure time were kept during the tests. As it is presented in Fig. 14, 64%, 62%, 60%, 55% and 47% efficiencies in 1, 2, 3, 4 and 5 recovering cycles were achieved.

4. Conclusions

We conducted the pilot experiment in a batch reactor to determine the IBP removal from the synthetic wastewater. The main results were summarized as follows:

- According to the BET theory, the surface areas of TiO_2 and m-TiO_2 were 110.5 and 43.5 m^2/g, respectively.
- N_2 adsorption analyses represented a pattern appertained to porous material.
- A high degradation of IBP was obtained at pH 7.
- The optimum IBP removal was achieved at 0.2 and 0.3 g of m-TiO_2 and TiO_2 by using LED lamps, respectively.
- The degradation efficiency of IBP increased as the IBP concentrations decreased. The most efficient concentration of IBP removal was achieved with 0.5 mg/l in the present study.
- IBP degradation persuades a Lagergren's first-order model, and rate constants of 0.123 and 0.0591 were obtained from kinetic study for m-TiO_2/LED and TiO_2/LED PCOs, respectively.
- A drop in removal performance of IBP from the synthetic wastewater by adding a radical scavenger occurred, which means the removal of IBP is based on the mechanism of hydroxyl radical.
- At the end of the study, we succeeded to remove the IBP from the synthetic wastewater with 91.26% and 52.4% efficiencies using m-TiO_2/LED and TiO_2/LED PCOs, respectively.

Conflict of Interest: None.

References

[1] P. Barnes, E. Griner, K. Fann, R. Nahin, Complementary and alternative medicine use among adults: United States, 2002, Seminars in Integrative Medicine, 2 (2004) 54–71.
[2] M. Klavarioti, D. Mantzavinos, D. Kassinos, Removal of residual pharmaceuticals from aqueous systems by advanced oxidation processes, Environ. Int., 35 (2009) 402–417.
[3] S. Mompelat, B. Le Bot, O. Thomas, Occurrence and fate of pharmaceutical products and by-products, from resource to drinking water, Environ. Int., 35 (2009) 803–814.
[4] L. Santos, A.N. Araujo, A. Fachini, A. Pena, C.D. Matos, M.C. Montenegro, Ecotoxicological aspects related to the presence of pharmaceuticals in the aquatic environment, J. Hazard. Mater., 175 (2010) 45–95.
[5] W. Sim, J. Lee, E. Lee, S. Shin, S. Hwang, J. Oh, Occurrence and distribution of pharmaceuticals in wastewater from households, livestock farms, hospitals and pharmaceutical manufactures, Chemosphere, 82 (2011) 179–186.
[6] E. Touraud, B. Roig, J. Sumpter, C. Coetsier, Drug residues and endocrine disruptors in drinking water: risk for humans?, Int. J. Hygiene Environ. Health, 214 (2011) 437–441.
[7] L. Heckmann, A. Callaghan, H. Hooper, R. Connon, H.T. Hutchinson, J.S. Maund, M.S. Richard, Chronic toxicity of ibuprofen to Daphnia magna: effects on life history traits and population dynamics, Toxicol. Lett., 172 (2007) 137–145.
[8] A. Nikolaou, S. Meric, D. Fatta, Occurrence patterns of pharmaceuticals in water and wastewater environments, Anal. Bioanal. Chem., 387 (2007) 1225–1234.
[9] T. Heberer, Tracking persistent pharmaceutical residues from municipal sewage to drinking water, J. Hydrology, 226 (2002) 175–189.
[10] S. Kim, J. Cho, I. Kim, B. Vanderford, S. Snyder, Occurrence and removal of pharmaceuticals and endocrine disruptors in South Korean surface, drinking, and waste waters, Water Res., 41 (2007) 1013–1021.
[11] G. Boyd, H. Reemtsma, D. Grimm, S. Mitera, Pharmaceuticals and personal care products (PPCPs) in surface and treated waters of Louisiana, USA, and Ontario, Canada, Sci. Total Environ., 311 (2003) 135–149.
[12] C. Yu, K. Chu, Occurrence of pharmaceuticals and personal care products along the West Prong Little Pigeon River in east Tennessee, USA, Chemosphere, 75 (2009) 1281–1286.
[13] P. Roberts, K. Thomas, The occurrence of selected pharmaceuticals in wastewater effluent and surface waters of the lower Tyne catchment, Sci. Total Environ., 356 (2006) 143–153.

[14] H.R. Buser, T. Poiger, M.D. Muller, Occurrence and environmental behavior of the chiral pharmaceutical drug ibuprofen in surface waters and in wastewater, Environ. Sci. Technol., 33 (1999) 2529–2535.
[15] C. Miege, J.M. Choubert, L. Ribeiro, M. Eusebe, M. Coquery, Removal efficiency of pharmaceuticals and personal care products with varying wastewater treatment processes and operating conditions—conception of a database and first results, Water Sci. Technol., 57 (2007) 49–56.
[16] S. Snyder, S. Adham, A. Redding, F. Cannon, J. Carolis, J. Oppenheimer, E. Wert, Y. Yoon, Role of membranes and activated carbon in the removal of endocrine disruptors and pharmaceuticals, Desalination, 202 (2006) 156–181.
[17] R. Giri, S. Ozaki, H. Ota, R. Takanami, S. Taniguchi, Degradation of common pharmaceuticals and personal care products in mixed solutions by advanced oxidation techniques, Int. J. Environ. Sci. Technol., 7 (2010) 251–260.
[18] H. Hossaini, G. Moussavi, M. Farrokhi, The investigation of the LED-activated FeFNS-TiO_2 nanocatalyst for photocatalytic degradation and mineralization of organophosphate pesticides in water, Water Res., 59 (2014) 130–144.
[19] R. Thiruvenkatachari, S. Vigneswaran, S. Moon, A review on UV/TiO2 photocatalytic oxidation process, Korean J. Chem. Eng., 25 (2008) 64–72.
[20] P. Dhiman, Mu. Naushad, K.M. Batoo, A. Kumar, S. Sharma, A.A. Ghfar, G. Kumar, M. Singh, Nano FexZn1−xO as a tuneable and efficient photocatalyst for solar powered degradation of Bisphenol A from water, J. Cleaner Prod., 165 (2017) 1542–1556.
[21] A. Kumar, Shalini, G. Sharma, Mu. Naushad, A. Kumar, S. Kalia, C. Guo, G.T. Mola, Facile hetero assembly of superparamagnetic Fe_3O_4/$BiVO_4$ stacked on biochar for solar photo-degradation of methyl paraben and pesticide removal from soil, J. Photochem. Photobiol. A: Chemistry, 337 (2017) 118–131.
[22] S.S. Bhande, R.B. Ambade, D.V. Shinde, S.B. Ambade, S.A. Patil, M. Naushad, R.S. Mane, Z.A. Alothman, S.-H. Lee, S.-H. Han, Improved photoelectrochemical cell performance of tin oxide with functionalized multiwalled carbon nanotubes–cadmium selenide sensitizer, ACS Appl. Mater. Interfaces, 7 (2015) 25094−25104.
[23] D. Pathania, D. Gupta, A.H. Al-Muhtaseb, G. Sharma, A. Kumar, Mu. Naushad, T. Ahamad, S.M. Alshehri, Photocatalytic degradation of highly toxic dyes using chitosan-g-poly (acrylamide)/ZnS in presence of solar irradiation, J. Photochem. Photobiol. A: Chemistry, 329 (2016) 61–68.
[24] P. Iovino, S. Chianese, S. Canzano, M. Prisciandaro, D. Musmarra, Degradation of ibuprofen in aqueous solution with UV light: the effect of reactor volume and pH, Water Air Soil Pollut., 2016 (2016) 194–227.
[25] J. Candido, S.J. Andrade, A.L. Fonseca, F.S. Silva, M.R.A. Silva, M.M. Kondo, Ibuprofen removal by heterogeneous photocatalysis and ecotoxicological evaluation of the treated solutions, Environ. Sci. Pollut. Res., 23 (2016) 19911–19920.
[26] J. Silva, J. Teodoro, R. Afonso, S. Aquino, R. Augusti, Photolysis and photocatalysis of ibuprofen in aqueous medium: characterization of byproducts via liquid chromatography coupled to high-resolution mass spectrometry and assessment of their toxicities against Artemia Salina, J. Mass Spectrom., 49 (2014) 145–153.
[27] H. Chen, Y. Ku, A. Irawan, Photodecomposition of o-cresol by UV-LED/TiO2 process with controlled periodic illumination, Chemosphere, 69 (2007) 156–181.
[28] F.S. Braz, M.R.A. Silva, F.S. Silva, S.J. Andrade, A.L. Fonseca, M.M. Kondo, Photocatalytic Degradation of Ibuprofen Using TiO_2 and Ecotoxicological Assessment of Degradation Intermediates against Daphnia similis, J. Environ. Protect., 5 (2014) 620–626.
[29] R. Vijayalakshmi, V. Rajendran, Synthesis and characterization of nano-TiO2 via different methods, Arch. Appl. Sci. Res., 4 (2012) 1183–1190.
[30] A. Zaleska, P. Górska, J.W. Sobczak, J. Hupka, Thioacetamide and thiourea impact on visible light activity of TiO_2, Appl. Catal. B: Environ., 76 (2007) 1–8.
[31] X. Yang, C. Cao, L. Erickson, K. Hohn, R. Maghirang, K. Klabunde, Photo-catalytic degradation of Rhodamine B on C-, S-, N-, and Fe-doped TiO2 under visible-light, irradiation, Appl. Catal. B: Environ., 91 (2009) 657–662.
[32] A.E. Giannakas, E. Seristatidou, Y. Deligiannakis, I. Konstantinou, Photocatalytic activity of N-doped and NeF co-doped TiO_2 and reduction of chromium(VI) in aqueous solution: an EPR study, Appl. Catal. B: Environ., 132 (2013) 460–468.
[33] M.S. Nahar, K. Hasegawa, S. Kagaya, Photocatalytic degradation of phenol by visible light-responsive iron-doped TiO2 and spontaneous sedimentation of the TiO2 particles, Chemosphere, 65 (2006) 1976–1982.
[34] Mu. Naushad, T. Ahamad, B.M. Al-Maswari, A. Alqadami, S.M. Alshehri, Nickel ferrite bearing nitrogen-doped mesoporous carbon as efficient adsorbent for the removal of highly toxic metal ion from aqueous medium, Chem. Eng. J., 330 (2017) 1351–1360.
[35] D. Pathania, G. Sharma, A. Kumar, Mu. Naushad, S. Kalia, A. Sharma, Z.A. ALOthman, Combined sorptional–photocatalytic remediation of dyes by polyaniline Zr(IV) selenotungstophosphate nanocomposite, Toxicol. Environ. Chem., 97 (2015) 526–537.
[36] S. Rajendran, D. Manoj, K. Raju, D.D. Dionysiou, Mu. Naushad, F. Gracia, L. Cornejo, M.A. Gracia-Pinilla, T. Ahamad, Influence of mesoporous defect induced mixed-valent NiO(Ni2+/Ni3+)-TiO_2nanocomposite for non-enzymatic glucose biosensors, Sensors Actuators B, 264 (2018) 27–37.
[37] D. Pathania, R. Katwal, G. Sharma, Mu. Naushad, M. Rizwan Khan, A.H. Al-Muhtaseb, Novel guar gum/Al_2O_3nanocomposite as an effective photocatalyst for the degradation of malachite green dye, Int. J. Biol. Macromol., 87 (2016) 366–374.
[38] A. Kumar, A. Kumar, G. Sharma, A.H. Al-Muhtaseb, Mu. Naushad, A.A. Ghfar, F.J. Stadler, Quaternary magnetic BiOCl/g-C_3N_4/Cu_2O/Fe_3O_4 nano-junction for visible light and solar powered degradation of sulfamethoxazole from aqueous environment, Chem. Eng. J., 334 (2018) 462–478.
[39] L.M. Bertus, R.A. Carcel, A. Duta, Prediction of TiO2 and WO3 nanopowders surface charge by the evaluation of point of zero charge (PZC), Environ. Eng. Manage. J., 10 (2011) 1021–1026.
[40] Pharmacopoeia Council of Europe, 6th ed., British Pharmacopoeia, London, 2009, pp. 3128–3136.
[41] D. Kanakaraju, B.D. Glass, M. Oelgemöller, Titanium dioxide photocatalysis for pharmaceutical wastewater treatment, Environ. Chem. Lett., 12 (2014) 27–47.
[42] I. Georgaki, E. Vasilaki, N. Katsarakis, A Study on the degradation of carbamazepine and ibuprofen by TiO_2 and ZnO photocatalysis upon UV/visible-light irradiation, Amer. J. Anal. Chem., 5 (2014) 518–534.
[43] M. Papamija, Photocatalytic degradation of ibuprofen using titanium dioxide, Boletín Técnico, 49 (2011) 35–40.
[44] Y. He, Photochemical Reactions of Naproxen, Ibuprofen and Tyrosine, Master Thesis, Purdue University, Indiana, 2013.
[45] M. Khaleghi Abbasabadi, S. Khodabakhshi, S. KianI, Titanium (IV) oxide nanoparticles: a green catalyst for the synthesis of dicoumarols in aqueous media, Proc. 5th International Congress on Nanoscience & Nanotechnology, Tehran, Iran, October 2014, pp. 22–24.